INVESTIGATION OF NONLINEAR BEHAVIOR OF T-SHAPED SHEAR WALLS

Ali Kheyroddin[1], Alireza Mortezaei[2]

[1]**Assistant Professor, Department of Civil Engineering, Engineering Faculty, Semnan University, Semnan, Iran**

[2]**M. Sc., Department of Civil Engineering, Engineering Faculty, Semnan University, Semnan, Iran**

mortezaei90@yahoo.com

Abstract: *Structural walls are used extensively in moderate- and high-rise buildings to resist lateral loads induced by earthquakes. The seismic performance of many buildings is, therefore, closely linked to the behavior of the reinforced concrete walls. The analytical models used in this paper are developed to study the push-over response of T-shaped reinforced concrete walls and investigate the influence of the flange walls on laterally loaded walls and nonlinear behavior of shear walls, namely strength, ductility and failure mechanisms. A layered nonlinear finite element method is used to study the behavior of T-shaped and rectangular (barbell) shear walls. This paper introduces a computer program to practically study three-dimensional characteristics of reinforced concrete wall response by utilizing layered modeling. The program is first verified by simulated and reported experimental response of 3-D reinforced concrete shear walls. Subsequently, a study considering eighteen analytical test specimens of T-shaped and barbell shear walls is carried out. Finally, based on analytical results, a new equation for minimum ratio of shear wall area to floor-plan area is proposed.*

Keywords: *Finite element method, T-shaped shear wall, Barbell shear wall, Ductility, Nonlinear analysis, Reinforced concrete.*

1. INTRODUCTION

In designing reinforced concrete (RC) frame-wall (or core) buildings, designers may choose "nonplanar" wall section, such as L, T, C etc., as opposed to "planar" shapes, such as rectangular or barbell.

Responses of nonplanar walls with at least one cross-sectional principal axis that is not a symmetry axis are typically governed by unsymmetrical bending and would be influenced by inelastic biaxial interaction more significantly than those of planar walls. A related problem arises in evaluating the seismic vulnerability of frame-wall construction possessing significant plan irregularity.

The use of nonlinear finite element (NLFE) analysis for the investigation of the strength and deformation properties of reinforced concrete (RC) structural walls has had limited success. Recent work, however, has indicated that the incorporation of a realistic model of concrete behavior into available well-established computer-based numerical techniques can yield close prediction of the response of reinforced concrete structural configurations.

2. RESEARCH SIGNIFICANT

Although the experimental data provide valuable information about the behavior of R.C. structure and observed hysteretic response, they are expensive and time-consuming and design procedures are not available to assist the engineer in designing of T-shaped shear walls. Using the nonlinear analysis method, it is now possible, at comparatively low cost and effort, to predict the complete response of more complex R.C. members and structures such as tall structural walls. In this paper, the first objective is to describe an analysis tool which is based on layered nonlinear finite element method (NONLACS2) and investigate nonlinear behavior of T-shaped shear walls. The second objective is to present an equation to calculate minimum ratio of T-shaped shear wall area to floor-plan area [1].

3. NONLINEAR FINITE ELEMENT PROGRAM

A nonlinear finite element analysis program, NONLACS2 (NONLinear Analysis of Concrete and Steel Structures), developed by Kheyroddin

[2], is used to analyze the selected R.C. shear walls. The program employs a layered finite element approach and can be used to predict the nonlinear behavior of any plain, reinforced or prestressed concrete, steel, or composite concrete-steel structure that is composed of thin plate members with plane stress conditions. This includes beams, slabs (plates), shells, folded plates, box girders, shear walls, or any combination of these structural elements. Time-dependent effects such as creep and shrinkage can also be considered.

3.1. Concrete properties

The concrete behaves differently under different types and combinations of stress conditions due to the progressive microcracking at the interface between the mortar and the aggregates (transition zone). The propagation of these cracks under the applied loads contributes to the nonlinear behavior of the concrete. As shown in Fig. 1(a), the uniaxial stress-strain curve of concrete adopted in this study, is made of two parts. The ascending branch up to the peak compressive strength is represented by the equation proposed by Saenz [3]:

$$\sigma = \frac{E_0 \varepsilon}{1 + \left(\frac{E_0}{E_{sc}} - 2\right)\left(\frac{\varepsilon}{\varepsilon_{max}}\right) + \left(\frac{\varepsilon}{\varepsilon_{max}}\right)^2} \quad (1)$$

Where E_0 is the initial modulus of elasticity of the concrete, E_{sc} is the secant modulus of the concrete at the peak stress, σ is stress, ε is strain and ε_{max} is the strain at peak stress. The descending or the strain-softening branch is idealized by the Smith and Young model [4]:
where σ_c is compressive strength of the concrete. For uniaxially loaded concrete, σ_c is equal to f'_c.

$$\sigma = \sigma_c \left(\frac{\varepsilon}{\varepsilon_{max}}\right) \exp\left(1 - \varepsilon / \varepsilon_{max}\right) \quad (2)$$

For analysis of most plane stress problems, concrete is assumed to behave as a stress-induced orthotropic material. In this study the orthotropic constitutive relationship developed by Darwin and Pecknold [5] is used for modelling the concrete using the smeared cracking idealization. The constitutive matrix, D, is given by:

$$D = \frac{1}{(1-\nu^2)} \begin{bmatrix} E_1 & \nu\sqrt{E_1 E_2} & 0 \\ \nu\sqrt{E_1 E_2} & E_2 & 0 \\ 0 & 0 & \frac{1}{4}(E_1 + E_2 - 2\nu\sqrt{E_1 E_2}) \end{bmatrix} \quad (3)$$

in which, E_1 and E_2 are the tangent moduli in the directions of the material orthotropy, and ν is the Poisson's ratio. The orthotropic material directions coincide with the principal stress directions for the uncracked concrete and these directions are parallel and normal to the cracks for the cracked concrete. The concept of the "equivalent uniaxial strain" developed by Darwin and Pecknold [5] is utilized to relate the increments of stress and strain in the principal directions. Therefore, stress-strain curves similar to the uniaxial stress-strain curves can be used to formulate the required stress-strain curves in each principal direction.

The strength of concrete, σ_c, and the values of E_1, E_2 and ν are functions of the level of stress, and the stress combinations. The concrete strength when subjected to biaxial stresses is determined using the failure envelope developed by Kupfer et al. [6]. The values of E_1 and E_2 for a given stress ratio ($\alpha=\sigma_1/\sigma_2$) are found as the slopes of the σ_1-ε_1 and σ_2-ε_2 curves, respectively. For the descending branches of both compression and tension stress-strain curves, E_i is set equal to a very small number, 0.0001, to avoid computational problems associated with a negative and zero values for E_i. The concrete is considered to be crushed, when the equivalent compressive strain in the principal directions exceeds the ultimate compressive strain of the concrete, ε_{cu}. For determination of the concrete ultimate compressive strain, ε_{cu}, two models for unconfined high and normal-strength concrete (Pastor [7]) and confined concretes (Scott et al. [8]) are implemented into the program.

For elimination of the numerical difficulties after crushing ($\varepsilon>\varepsilon_{cu}$) and cracking of the concrete ($\varepsilon>\varepsilon_{tu}$), a small amount of compressive and tensile stress as a fraction of concrete strength, $\gamma_c f'_c$ and $\gamma_t f'_t$, is assigned (optional) at a high level

of stress (Fig. 1(a)), where parameters γ_c and γ_t define the remaining compressive and tensile strength factors, respectively.

3.2. Crack Modelling Techniques

Cracking of the concrete is one of the important aspects of material nonlinear behavior of the concrete. Besides reducing the stiffness of the structure, cracks have resulted in redistribution of stresses to the reinforcing steel as well as increasing the bond stress at the steel-concrete interface. Cracking of the concrete is idealized using the fixed smeared cracking model and is assumed to occur when the principal tensile stress at a point (usually a Gauss integration point) exceeds the tensile strength of the concrete. After cracking, the axes of orthotropy are aligned parallel and orthogonal to the crack. The elastic modulus perpendicular to the crack direction is reduced to a very small value close to zero and the Poisson effect is ignored. The effect of the crack is smeared within the element by modifying the [D] matrix. If σ_1 exceeds the tensile strength of concrete, f'_t, the material stiffness matrix is defined as (one crack is opened):

$$[D] = \begin{bmatrix} 0 & 0 & 0 \\ 0 & E_2 & 0 \\ 0 & 0 & \beta G \end{bmatrix} \quad \text{Where } 0<\beta\leq 1.0 \qquad (4)$$

Once one crack is formed, the principal directions are not allowed to rotate and a second crack can form only when $\sigma_2 > f'_t$, in a direction perpendicular to the first crack. Then,

$$[D] = \begin{bmatrix} 0 & 0 & 0 \\ 0 & 0 & 0 \\ 0 & 0 & \beta G \end{bmatrix} \quad \text{Where } 0<\beta\leq 1.0 \qquad (5)$$

The shear retention factor, β, with a value of less than unity, serves to eliminate the numerical difficulties that arise if the shear modulus is reduced to zero, and more importantly, it accounts for the fact that cracked concrete can still transfer shear forces through aggregate interlock and dowel action. Due to the bond between the concrete and the steel reinforcement, a redistribution of the tensile stress from the concrete to the reinforcement will occur. In fact, the concrete is able to resist tension between the cracks in the direction normal to the crack; this phenomenon is termed tension-stiffening. The tension-stiffening effect is idealized by assuming the ascending and the descending branches of the tensile stress-strain curve to terminate at ε_{cr} and ε_{tu}, respectively. For evaluation of an "appropriate" value of the ultimate tensile strain of the concrete, ε_{tu}, and elimination of mesh size dependency phenomenon, Shayanfar et al [9] proposed the following simple formula:

$$\varepsilon_{tu} = 0.004\ e^{-0.008\ h} \quad (\ \varepsilon_{tu} \geq \varepsilon_{cr}) \qquad (6)$$

where h is the width of the element in mm and ε_{cr} is the concrete cracking strain. For elimination of the element size effect phenomenon, both the new proposed model and the crack band model, based on fracture mechanics, proposed by Bazant and Oh [10] have been implemented into the NONLACS2 program [2].

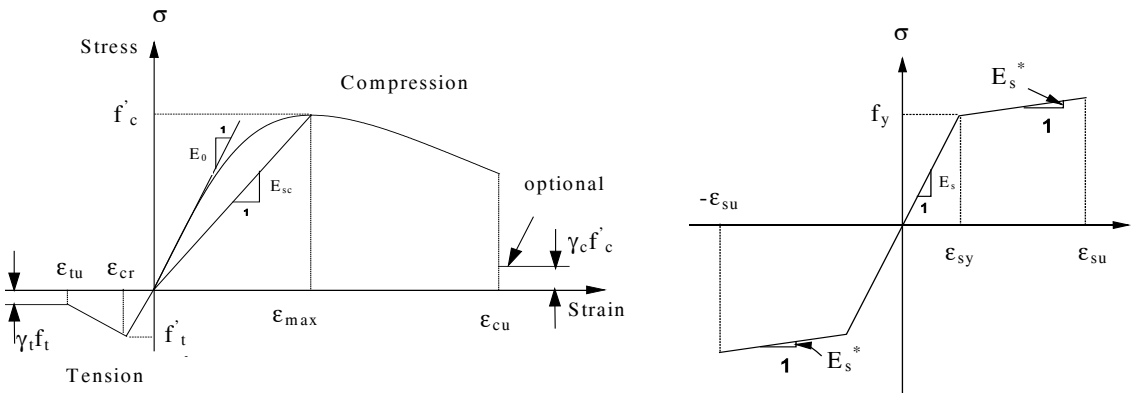

Fig. 1 - Uniaxial stress-strain curves, a) Plain Concrete, b) Steel Reinforcement

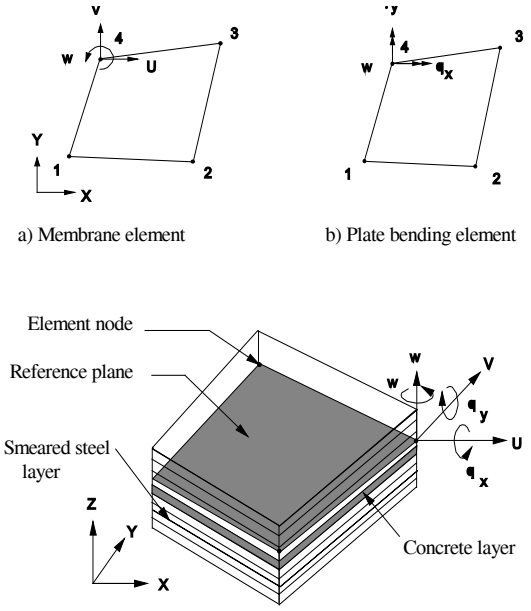

Fig. 2. Some typical finite elements in NONLACS2 Program [2]

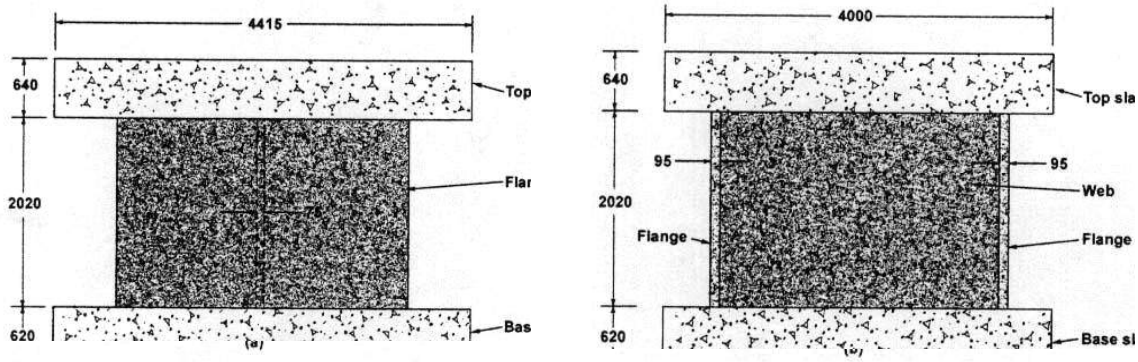

Fig. 3. Test specimen details: (a) end view; (b) side view. [11]

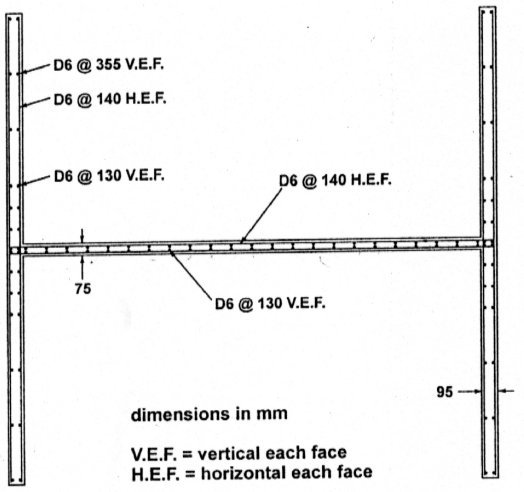

Fig. 4. Top view of wall reinforcement [11]

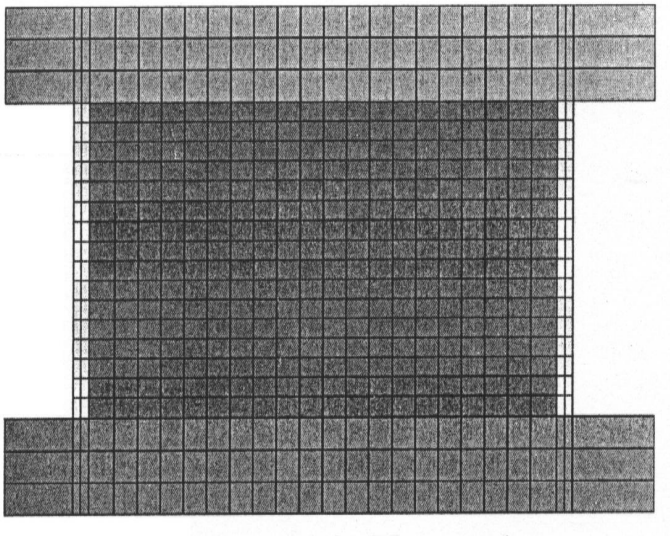

Fig. 5. Finite element mesh configuration

3.3. Reinforcing bar properties

The reinforcing bars are modeled as an elastic strain-hardening material as shown in Fig. 1(b). The reinforcing bars can be modeled either as smeared layers or as individual bars. In both cases, perfect bond is assumed between the steel and the concrete.

3.4. Finite element formulation

The element library includes plane membrane, plate bending, one dimensional bar, shear connecter, spring boundary elements as well as a facet shell element, which is a combination of the plane membrane and the plate bending elements. Figure 2 shows some of these elements and the associated degrees of freedom. The two nodes, three degrees of freedom per node one dimensional bar element is used to model uniaxial truss members, unbonded prestressed tendons and shear connectors. The program employs a layered finite element approach.

The structure is idealized as an assemblage of thin constant thickness plate elements with each element subdivided into a number of imaginary layers as shown in Fig. 2(c). A layer can be either of concrete, smeared reinforcing steel or a continuous steel plate. The number of layers depends on the behavior of the structure being analyzed. Each layer is assumed to be in a state of plane stress, and can assume any state-uncracked, partially cracked, fully cracked, non-yielded, yielded and crushed -depending on the stress or strain conditions.

3.5. Nonlinear analysis method

Analysis is performed using an incremental-iterative tangent stiffness approach. , and the element stiffness is obtained by adding the stiffness contributions of all layers at each Gauss quadrature point. The change in the material stiffness matrix during loading necessitates an incremental solution procedure with a tangent stiffness scheme that using piece-wise linearization has been adopted in the NONLACS2 program

4. VERIFICATION OF NONLACS2

The capability of NONLACS2 program to reliably simulate the fundamental behavior arising from elastic and inelastic flexure interaction was verified by correlating analytically simulated and measured response of two works. In each case, different forms of output (including mode of failure) were extracted and compared with experimental results to verify key aspects of the numerical model. Although some discrepancies were observed, the overall match between the analytical models and experimental tests was good.

4.1. Vecchio and Palermo flanged walls

Two large-scale flanged shear walls tested under static cyclic displacement by Palermo and Vecchio (2002) [11]. The specimens were constructed with stiff top and bottom slabs. The top slabs (4415×4000×640 mm) served to

distribute the horizontal and axial load to the walls of the structure. The bottom slab (4415×4000×620 mm), clamped to the laboratory strong floor, simulated a rigid foundation. The slabs were reinforced with NO.30 (29.9 mm) deformed reinforcing bars at a spacing of 350 mm in each direction, with a top and bottom layer. The web wall, 2885 mm in length, 2020 mm in height, and 75 mm in thickness, was reinforced with D6 reinforcing bars, the bars were spaced 140 mm horizontally and 130 mm vertically in two parallel layers. The two flange walls were approximately 3045 mm long, 2020 mm high, and 95 mm thick. The flanges were also reinforced with D6 reinforcing bars, spaced 140 mm horizontally and 130 mm vertically near the web wall and 255 mm near the tips of the flanges. The concrete clear covers in the walls and slabs were 15 and 50 mm, respectively. Dimensional details of the walls are shown in Fig. 3 and the reinforcement layout for the web and flange walls are given in Fig. 4. The two shear walls had identical dimensions and reinforcement, and details of the concrete and reinforcement properties are given in Table 1 and 2, respectively. A two-dimensional static monotonic analysis was performed by Vecchio [12]. The finite element mesh, shown in Fig.5, consisted of 540 constant strain rectangular elements.

Table 1. Concrete material properties [11]

Zone	f'_c , MPa		ε_c , MPa($\times 10^{-3}$)	
	DP1	DP2	DP1	DP2
Web Wall	21.7	18.8	2.04	2.12
Flange Wall	21.7	18.8	2.04	2.12
Top Slab	43.9	38.0	1.93	1.96
Bottom Slab	34.7	34.7	1.66	1.66

Table 2. Reinforcement material properties [11]

Zone	Type	Diameter (mm)	ε_{sy} ($\times 10^{-3}$)	f_{sy} MPa	f_{su} MPa
Web Wall	D6	7	3.18	605	652
Flange Wall	D6	7	3.18	605	652
Top Slab	No. 30	29.9	2.51	550	696
Bottom Slab	No. 30	29.9	2.51	550	696

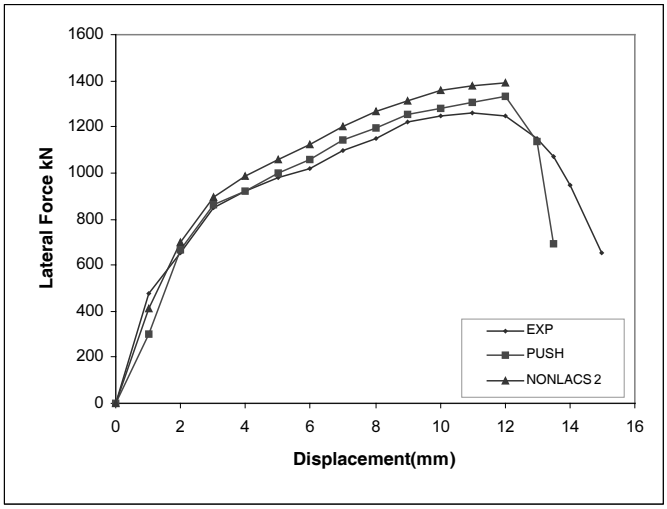

Fig. 6. Comparison of experimental and analytical results

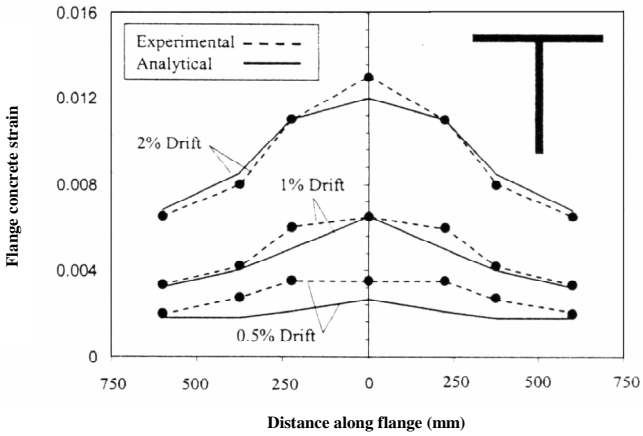

Fig. 7. Measured and computed tension flange strain profile for Specimen TW2

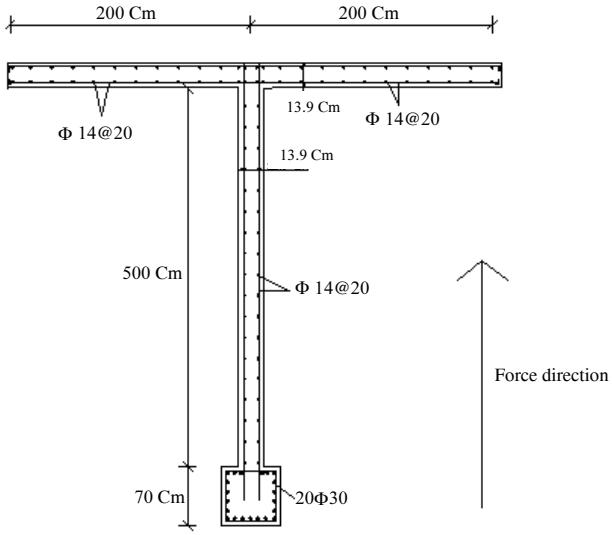

Fig. 8. Reinforcing details of T-shape shear wall with compressed flange

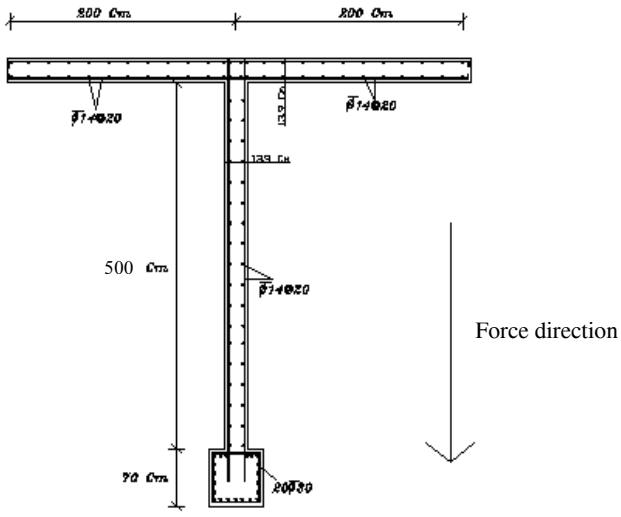

Fig. 9. Reinforcing details of T-shape shear wall with tension flange

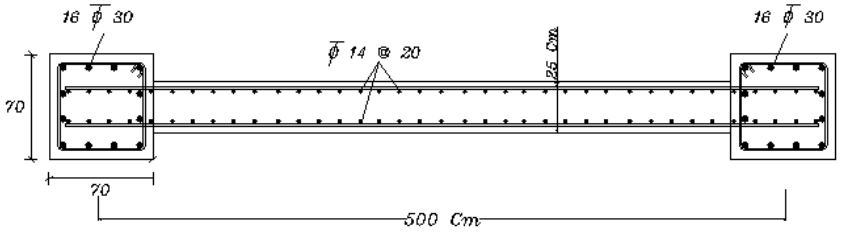

Fig. 10. Reinforcing details of barbell shear wall

The mesh was divided into four zones: the web wall, flange walls, top slabs, and bottom slabs. Lateral load was imposed on the top-right joint and the axial load was spread along the top rows of joint. For modeling of I-shaped shear wall in NONLACS2 program, have been used four-node shell elements, QLC3 type as plane stress and bending. Results analyses are plotted in Fig.6 along with the envelope response of the two-dimensional pushover analysis and the experimental response of the specimen. The result indicated that NONLACS2 programs provide reasonable results and can be used to approximate ultimate load. An ultimate load of 1390 KN was reported for shear wall.

4.2. Wallace and Thomsen flanged walls

Wallace and Thomsen [13] conducted tests of T-shaped RC walls subjected to axial compression and cyclic lateral loading. Using measured material properties and dimensions, the monotonic and cyclic responses of Wall TW2 are calculated and compared with the test results. The measured and calculated load-deflection curves match well. As shown in Fig. 7, the measured strain distribution in the flange under tension also compares well to the computed strains for various drift levels. Because the model cannot capture local bar buckling , it was unable to predict the initiation of these modes of failure as observed in the tests. Nevertheless, the analytical results correlate well to the test data prior to the occurrence of these local modes of failure.

5. STUDY OF NONLINEAR BEHAVIOR OF SHEAR WALLS

Analytical specimens comprised T-shaped and barbell walls with similar cross section. Both shear walls are to be constructed in Iranian Concrete Code (ABA). T-shaped shear walls were modeled using four-node isoparametric plane-stress elements as RQUAD4 that have good behavior for three-dimensional walls.

The web wall, 500 cm in length, 13.9 cm in thickness, 3000 cm in height for 10-story walls, 6000 cm for 20-story walls and 9000 cm for 30-story walls, was reinforced with Φ10 reinforcing bars. The bars were spaced 25 cm horizontally and vertically in two parallel layers. The flange wall was 400 cm long and 13.9 cm thick. The flange was reinforced with Φ14 reinforcing bars, spaced 20 cm horizontally and vertically. Totally the mesh configuration of these shear walls consisted of 360 elements and 403 joints that these elements were 100 cm high and 50 cm long or 100 cm high and 100 cm long. Lateral loads were imposed spread in 30 steps. Reinforcement was applied smeared layer and totally four layers have been used in different zones. Dimensional details of the walls and reinforcement layout are given in Fig. 8 and 9 for T-shaped walls with compressed flange and T-shape walls with tensiled flange, respectively. Comprehensive material properties of T-shaped with compressed flange and T-shaped walls with tensile flange are given in Table 3 and 4, respectively.

Barbell shear walls were modeled using four-node plane-stress elements as QLC3 that have good behavior for three-dimensional walls. Walls were 500 cm long, 25 cm thick, 3000 cm high for 10-story walls, 6000 cm high for 20-story walls and 9000 cm high for 30-story walls. Shear walls were reinforced with Φ14 at the web and 16Φ30 at the tips of walls. Totally, the model of these shear walls consisted of 180 elements and 217 joints. Lateral loads were imposed spread in 30 steps. Reinforcement was applied individual bars and smeared layer that totally four layers have been used in different zone. Dimensional details, reinforcement layout and material properties of barbell shear walls are given in Fig. 10 and Table 5, respectively.

Table 3. Material properties of T-shape shear walls with compressed flange

Name	TS101	TS102	TS103	TS201	TS202	TS203	TS301
Type of wall	T-Shaped	T-Shaped	T-Shaped	T-Shaped	T-Shaped	T-Shaped	T-Shaped
Wall height (m)	30	30	30	30	30	30	30
$f_c^{'}$ (N/mm^2)	20	20	20	20	20	20	20
ε_{c0}	0.002	0.002	0.002	0.002	0.002	0.002	0.002
ε_{cu}	0.003	0.003	0.003	0.003	0.003	0.003	0.003
ε_{tu}	0.00013	0.00013	0.00013	0.00013	0.00013	0.00013	0.00013
f_y (N/mm^2)	400	400	400	400	400	400	400
E_s (kN/mm^2)	210	210	210	210	210	210	210
ε_{su}	0.04	0.04	0.04	0.04	0.04	0.04	0.04
Final load step	16	15	28	8	30	19	18
Ultimate displace-ment (mm)	999.92	1126.7	1263.1	1649	4347.5	3643.6	7884.6
Ultimate load (kN)	1500	1400	1500	700	900	850	800

Table 4 – Material properties of T-shape shear walls with tension flange

Name	ITS101	ITS102	ITS201	ITS202	ITS301
Type of wall	T-Shaped	T-Shaped	T-Shaped	T-Shaped	T-Shaped
Wall height (m)	30	30	30	30	30
$f_c^{'}$ (N/mm^2)	20	20	20	20	20
ε_{c0}	0.002	0.002	0.002	0.002	0.002
ε_{cu}	0.003	0.003	0.003	0.003	0.003
ε_{tu}	0.00013	0.00013	0.00013	0.00013	0.00013
f_y (N/mm^2)	400	400	400	400	400
E_s (kN/mm^2)	210	210	210	210	210
ε_{su}	0.04	0.04	0.04	0.04	0.04
Final load step	13	26	8	17	12
Ultimate displace-ment (mm)	163.26	175.86	649.59	736.91	1470.9
Ultimate load (kN)	1200	1260	700	750	550

T-shaped and rectangular shear walls discussed in this paper were analysis by NONLAC2 program and results have been showed in Figs. 11, 12 and 13. Figs. 11, 12 and 13 plot load-displacement relationship for shear walls in 10-story, 20-story and 30-story building. The results of the analysis demonstrate when flange wall is under the compression; wall shows higher strength rather than barbell wall and wall with tension flange. For instance, the ultimate load of T-shaped shear wall with compressed flange is 1500 kN that this value is 1.2 times shear wall strength with tension flange (1200 kN) and 1.76 times barbell shear wall strength (2000 kN). Comparison of lateral displacement of shear walls show that T-shape shear wall with compressed flange have better displacement ductility than T-shaped wall with tension flange.

Table 5 - Material properties of barbell shear walls

Name	RS101	RS102	RS103	RS201	RS202	RS301
Type of wall	Rectangular	Rectangular	Rectangular	Rectangular	Rectangular	Rectangular
Wall height (m)	30	30	30	30	30	30
f_c' N/mm^2	20	20	20	20	20	20
ε_{c0}	0.002	0.002	0.002	0.002	0.002	0.002
ε_{cu}	0.003	0.003	0.003	0.003	0.003	0.003
ε_{tu}	0.00013	0.00013	0.00013	0.00013	0.00013	0.00013
f_y N/mm^2	400	400	400	400	400	400
E_s kN/mm^2	210	210	210	210	210	210
ε_{su}	0.04	0.04	0.04	0.04	0.04	0.04
Final load step	9	7	29	6	24	22
Ultimate displace-ment (mm)	206.63	319.89	278.08	769.72	1014	1893.8
Ultimate load (kN)	800	600	900	500	560	520

Table 6 – Simplify proposed equation

h_w/l_w	ρ_{min}
2.00	0.0031
2.67	0.0050
3.00	0.0060
4.00	0.0094
5.00	0.0132
5.33	0.0145
6.00	0.0171
6.67	0.0199
7.00	0.0213
8.00	0.0256
9.00	0.0300
10.00	0.0345

For instance, when flange is in compression, wall displacement ductility is 10.41 that approximately 5.2 times barbell shear wall ductility.

The mechanism leading to failure for barbell shear wall and T-shaped wall with compressed flange was initiated by yielding of the flexural reinforcement but in T-shaped wall with tension flange, failure was initiated by crushing of the concrete without any yielding of the reinforcement. Therefore, barbell shear wall and T-shaped wall with compressed flange have flexural failure but T-shaped wall with tension flange have brittle failure. By the way, the analytical results show that T-shaped shear wall when the flange is in tension have no ductility, namely the shear wall have brittle failure mechanism. Comparison of cracking load shows that when the flange of T-shaped wall is in tension, the wall shows higher strength compared with barbell shear wall and shear wall with compressed flange. Because, the stiff flange walls provided restraint against the diagonal cracks in the web wall.

6. PROPOSED EQUATION

Postanalysis investigations have revealed that estimation for number of shear walls on the building is required. It is often desirable to develop simplified expression that can be used for rapid evaluation. The primary variables affecting wall deformation capacity were identified to be the ratio of wall cross-sectional area to the floor-plan area. Thomsen and Wallace [13] developed an expression for symmetrically reinforced walls with a rectangular cross section (see Eq. 7). In addition

to presenting simplified rules to establish cases where special transverse reinforcement is not required, a conservative approach to determine the amount of shear walls is presented. Therefore in the shear wall building by this equation can estimate number of shear walls. This causative is that designer must adopt good arrangement for the walls. The result is expressed as

$$\rho_{\min} = \frac{\left(\frac{h_w}{l_w}\right)^2}{865 + 160\frac{h_w}{l_w} + 7.4\left(\frac{h_w}{l_w}\right)^2} \approx \frac{\left(\frac{h_w}{l_w}\right)^2}{900 + 200\frac{h_w}{l_w}} \quad (7)$$

Where ρ_{min} = the minimum ratio of wall area to floor-plan area; h_w = wall height; and l_w = wall length (that is average length of shear walls in plan). For simplicity, Eq. 7 are given in Table 6 based on h_w/l_w. According to the nonlinear results of T-shaped shear walls and development of axial force-moment interaction curves for increase the minimum ratio of shear wall area to floor-plan area for T-shaped shear walls buildings, so that Eq. 7 becomes :

$$\rho_{\min} = K\frac{\left(\frac{h_w}{l_w}\right)^2}{900 + 200\frac{h_w}{l_w}} \quad (8)$$

That

$$K = e^{\left(-0.5246 + 4.9988 * 10^{-7} h^3{}_w\right)} \quad (9)$$

Table Curve program was used for calculating the decay factor, K. Among 107 equations that were proposed by program, one equation that has high accuracy was selected.

Two types of exercises were carried out to verify the accuracy of the developed equation. First, convergence studies were carried out to determine the number of T-shaped shear walls for producing reasonable results.

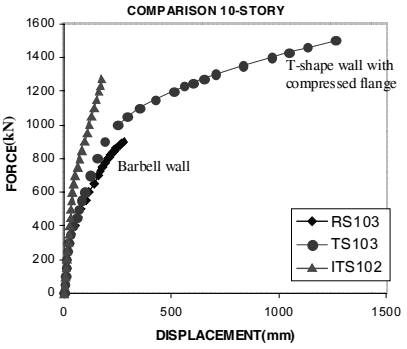

Fig. 11. Load-displacement relationship for 10-story shear wall

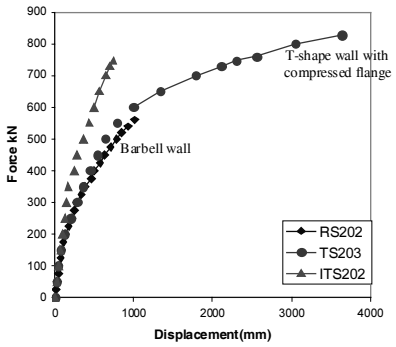

Fig. 12. Load-displacement relationship for 20-story shear wall

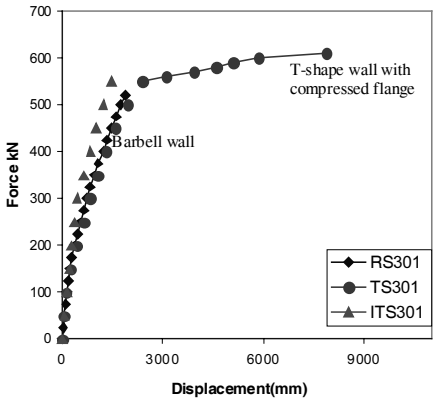

Fig. 13. Load-displacement relationship for 30-story shear wall

Then, to determine if the models are capable of faithfully reproducing wall behavior, analytical results were compared with results in Ngwenya [14]. The results of comparison indicated that Eq. 2 provide reasonable results and can be used to approximate the number of T-shaped shear walls.

7. SUMMARY AND CONCLUSIONS

The analytical results of the shear walls provide detailed information about the behavior of T-shaped shear walls and influence of applying flange. T-shape reinforced concrete walls subjected to lateral load exhibit types of response that are not considered in building codes, such as increasing of strength and ductility. The analytical models discussed in this paper are capable of reproducing the important features of the measured push-over response of T-shape shear walls.

The results of these analyses indicate that the push-over response of the barbell walls can be improved by using T-shape shear wall with the same area. Adding the flange improves the response significantly because the flange carries main parts of forces and behave in 3-dimensional mode. When T-shape shear walls flange is pushed, shear walls show high ductility, also a T-shape shear wall have a high lateral strength rather than rectangular shear walls and T-shape shear wall with tension flange, and cause decreasing of displacement at top stories of building. The stiffness of the flange walls was largely responsible for the mode of failure. According three-dimensional performance of T-shape shear walls, they can be used in two direction of building as a lateral resistant system.

REFERENCES

[1] Mortezaei, A.R., “Investigation of Linear and Nonlinear Behavior of T-Shaped Shear Walls”, M. Sc. Thesis, Department of Civil Engineering, Engineering Faculty, Semnan University, Semnan, Iran, July 2003, 240p.

[2] Kheyroddin, A., "Nonlinear Finite Element Analysis of Flexure-Dominant Reinforced Concrete Structures", Ph.D. Thesis, Department of Civil Engineering and Applied Mechanics, McGill University, Montreal, Canada, March 1996, 290p.

[3] Saenz, L.P., "Equation for the Stress-Strain Curve of Concrete in Uniaxial and Biaxial Compression of Concrete", ACI Journal, V. 61, No. 9, 1965, pp. 1229-1235.

[4] Smith, G. M., and Young, L. E., "Ultimate Theory in Flexure by Exponential Function", ACI Journal, V. 52, No. 3, 1955, pp. 349-359.

[5] Darwin, D., and Pecknold, D.A., "Nonlinear Biaxial Stress-Strain Law for Concrete", ASCE Journal of the Engineering Mechanics Division, V. 103, No. EM4, 1977, pp. 229-241.

[6] Kupfer, H. B.; Gerstle, K. H. and Rusch, H., "Behavior of Concrete Under Biaxial Stresses," ACI Journal, V. 66, No. 8, 1969, pp. 656-666.

[7] Pastor, J.A., "High-Strength Concrete Beams", Ph.D. Thesis, Cornell University, New York, Ithaca, 1986.

[8] Scott, B.D., Park, R., and Priestly, M.J.N., "Stress-Strain Behavior of Concrete Confined by Overlapping Hoops at Low and High Strain Rates", ACI Journal, V. 79, No. 1, Jan./Feb. 1982, pp. 13-27.

[9] Shayanfar, M.A.; Kheyroddin, A.; and Mirza, M.S., "Element Size Effects in Nonlinear Analysis of R.C. Members", Computer & Structure, Vol.62, No.2, 339-352 (1997).

[10] Bazant, Z. P., and Oh, B.H., "Crack Band Theory for Fracture of Concrete", Material and Structures, V. 16, No. 93, 1983, pp. 155-177.

[11] Vecchio, F.J., Palermo, D., “Behavior of Three Dimensional Reinforced Concrete Shear Walls”, ACI Structural Journal, Vol.99, No.1, Jan.-Feb. 2002.

[12] Vecchio, F.J., “Towards Cyclic Load Modeling of Reinforced Concrete”, ACI Structural Journal, Vol.96, No.2, Mar.-Apr. 1999, pp.389-407.

[13] Wallace, J.W., Thomsen, J.H. “Seismic Design of RC Structural Walls”, ASCE Journal of Structural Engineering, Vol.121, No.1, January, 1995, pp. 88-101.

[14] Ngwenya, B., (1996), "Nonlinear Analysis of High-Rise Structural Walls", M. Sc. Thesis, Department of Civil Engineering and Applied Mechanics, McGill University, Montreal, Canada.
[15] Vecchio, F.J., "Lesson From the Analysis of a Three Dimensional Concrete Shear Wall", Structural Engineering and Mechanics, Vol.6, No.4, 1998, pp. 439-455.
[16] Lefas, I.D., Kotsovos, M.D., and Ambraseys, N.N. (1990) "Behavior of Reinforced Structural Walls : Strength Deformation Characteristics and Failure Mechanics", ACI Structural Journal, 87(S3), pp.23-31.
[17] Lefas, I.D., Kotsovos, M.D., (1990) "NLFE Analysis of RC Structural Walls and Design Implications", ASCE Journal of Structural Engineering, 116(1), pp.146-165.
[18] Collins, Michael P., "Toward a Rational Theory for RC Members in Shear", Proceeding, ASCE, Vol.104, ST4, Apr.1978, pp.649-666.
[19] ACI Committee 318, "Building Code Requirements for Reinforced Concrete (ACI 318-83)", American Concrete Institute, Detroit, 1983, 111pp.
[20] Huria, V., Raghavendrachar, M., Aktan, A., (1991) "3-D Characteristics of RC Wall Response", ASCE Journal of Structural Engineering, Vol.117, No.10, pp.3149-3167.
[21] Wallace, J.W., (1992) "BIAX revision1: a Computer Program for the Analysis of Reinforced Concrete and Reinforced Masonry Sections", Rep. No. CU/CEE-92/4, Department of Civil and Environmental Engineering, Clarkson University, Potsdam, N.Y.
[22] American Concrete Institute (1995), Standard Building Code Requirements for Reinforced Concrete, ACI 318-95, and Detroit: ACI.